25th ABCM International Congress of Mechanical Engineering
October 20-25, 2019, Uberlândia, MG, Brazil

A MODEL OF A LINEAR PERMANENT MAGNET ALTENATOR FOR DESIGN AND OPTIMIZATION: PART II. PARAMETRIC ANALYSIS

Roger Victor Rodrigues *
Marcelo Braga dos Santos *
Laboratório de Sistemas Mecânicos
rogervrodrigues@gmail.com
marcelo.bragadossantos@ufu.br

Solidônio Rodrigues de Carvalho *
Laboratório de Transferência de Calor e Massa
solidonio@ufu.br

*Universidade Federal de Uberlândia

Abstract. *This paper presents a parametric analysis of a numerical model, built for design and optimization purposes, in order to understand and verify how the electromechanical efficiency of the generator is affected by the electrical and mechanical parameters of the system. The efficiency of the generator is estimated by the results obtained via numerical integration of the EDO system that describes the dynamical behavior of the system. A stronger influence of the electrical parameters on the generators efficiency is noticed. In contrast, different values of the natural frequency of the mechanical system leaded to variations smaller than 1.5 %. Also, a comparison between the results obtained for the different electrical circuit models is done.*

Keywords: *energy convertion, parametric analysis, tubular generator*

1. INTRODUCTION

Parametric analysis is powerful source which can lead to a wider comprehension of the system, and thus give the sufficient knowledge basis, with which is possible to trace the better strategical ways to obtain the best performance and design of a certain equipment. It can also provide informations with which control strategy would be obtained.

This paper presents the results of the parametric analysis of a numerical model built for design and optimization purposes. It is observed how the electromechanical efficiency of the generator is affected by the variation of the electrical and mechanical parameters of the system. Also, a comparison between the results obtained for the different electrical circuit models is done.

2. MODEL DESCRIPTION

The numerical model primarily aims to describe the translator motion which is governed by Newton's second law. The forces acting upon the linor are mechanical friction forces, the electromagnetic force due to the linear alternator and the excitation force. To accordingly represent these phenomena, a 1 degree of freedom (1 DOF) vibratory system is chosen as model, as illustrated in Fig. 1.

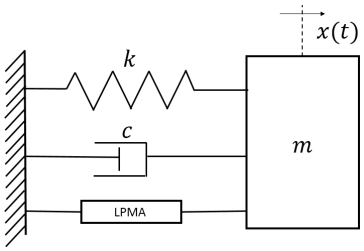

Figure 1. Schematic diagram of the dynamical model.

In order to accordingly represent the phenomena of dynamical and electromagnetical natures, two sub-models developed: the dynamical model and the Linear Permanent Magnet Alternator model. Figure 2 illustrates the relation between

these models and the input and output variables.

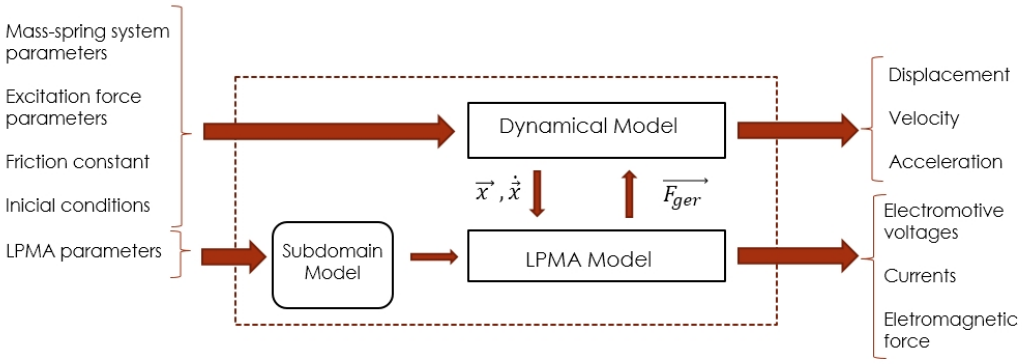

Figure 2. Diagram of the simulation model

The electromotive voltage at the "*i-th*" coil can be calculated with the Eq. (1).

$$e_i(t) = -N_c \frac{d\Lambda_{i,pm}(x)}{dt} = -N_c \frac{d\Lambda_{i,pm}(x)}{dx}\frac{dx}{dt} \tag{1}$$

Where $\Lambda_{i,pm}(x)$ is the flux linkage at the coil "*i-th*" due to the magnets and N_c is the number of turns of the coils. To estimate the flux linkage $\Lambda_{i,pm}$ the Subdomain Method was chosen. The details of this method are available in (Rodrigues *et al.*, 2019).

Equation (2) shows the expression by which the electromagnetic force can be calculated.

$$F_{ger} = N_c \cdot N_{pa} \begin{Bmatrix} i_A & i_B & i_C \end{Bmatrix} \frac{d}{dx} \begin{Bmatrix} \Lambda_{A,pm}(x) \\ \Lambda_{B,pm}(x) \\ \Lambda_{C,pm}(x) \end{Bmatrix} \tag{2}$$

Where $\Lambda_{a,pm}(x)$ are the flux linkage at the phase "a" due to the magnets, N_{pa} is the number of active parts of the LPMA and i_a are the instantaneous current for the phase "a".

Figure 3 illustrates the schematic diagram of the electrical circuit of the alternator for the phase A, considering that the load of this equipment is a resistor $R_{L,A}$.

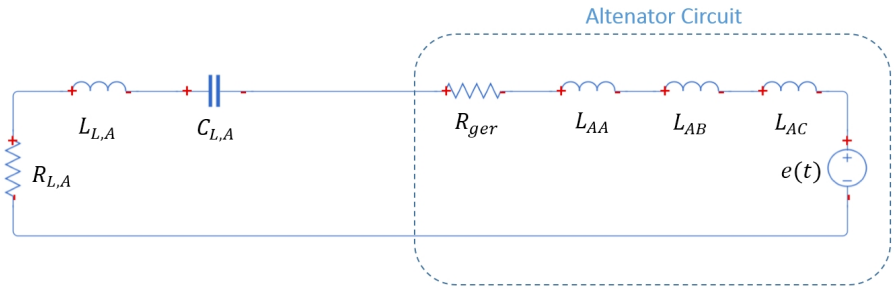

Figure 3. Schematic diagram of the electrical circuit of the alternator for the phase A.

In this model, the resistance, the self- and the mutual inductance of the LPMA are considered. Also the possibility to add an inductance $L_{L,A}$ and a capacitor $C_{L,A}$ in the external circuit exists. Therefore, three models were elaborated in this work namelly R-, RL- and RLC model.

The R model is written considering that both inductance and capacitance of the circuit are neglectable. In that case, the Eq. (3) can be directly solved, considering that the electromotive voltage, the induced current, and therefore the electromagnetic force are fully determined by Eq. (1), (4), and (2), respectively.

$$\begin{Bmatrix} \ddot{x}(t) \\ \dot{x}(t) \end{Bmatrix} = \begin{bmatrix} 1/m & 0 \\ 0 & 1/c \end{bmatrix} \left(\begin{bmatrix} c & k \\ -c & 0 \end{bmatrix} \begin{Bmatrix} \dot{x}(t) \\ x(t) \end{Bmatrix} + \begin{Bmatrix} F(t) - F_{ger}(t) \\ 0 \end{Bmatrix} \right) \tag{3}$$

Where m, c and k are the parameters of the mass-spring system – mass, damping and stiffness coefficient, respectively. $F(t)$ and $F_{ger}(t)$ are the excitation and electromagnetic forces.

$$\{i(t)\} = [R_T]^{-1}\{e(t)\} \tag{4}$$

Where $[R_T]$ is $3x3$ diagonal matrix that each element is relative to the resultant resistance for the respective phase circuit.

The RL model is built considering that only the capacitance of the circuit is null. If one determines to solve a system using a RL model, then Equation (5) must be solved.

$$\begin{Bmatrix} \ddot{x}(t) \\ \dot{x}(t) \\ \{\dot{i}(t)\} \end{Bmatrix} = \begin{bmatrix} m & 0 & \{0\} \\ 0 & c & \{0\} \\ \{0\} & \{0\} & -[L_T] \end{bmatrix}^{-1} \left(\begin{bmatrix} c & k & \{0\} \\ -c & 0 & \{0\} \\ \{0\} & \{0\} & [R_T] \end{bmatrix} \begin{Bmatrix} \dot{x}(t) \\ x(t) \\ \{i(t)\} \end{Bmatrix} + \begin{Bmatrix} F(t) - F_{ger}(t) \\ 0 \\ \{e(t)\} \end{Bmatrix} \right) \tag{5}$$

Where $F_{ger}(t)$ and $e(t)$ are determined by solving Eq. (2) and Eq. (1), respectively.

In the third model – RLC model – all the electrical components shown in the schematic diagram are considered relevant to the dynamical response of the system. In case that one chooses to apply the RLC model, the EDO indicated in the Eq. (6) must be solved.

$$\begin{Bmatrix} \ddot{x}(t) \\ \dot{x}(t) \\ \{\dot{i}(t)\} \\ \{\dot{q}(t)\} \end{Bmatrix} = \begin{bmatrix} m & 0 & \{0\} & \{0\} \\ 0 & c & \{0\} & \{0\} \\ \{0\} & \{0\} & [L_T] & [0] \\ \{0\} & \{0\} & [0] & [R_T] \end{bmatrix}^{-1} \left(\begin{bmatrix} c & k & \{0\} & \{0\} \\ -c & 0 & \{0\} & \{0\} \\ \{0\} & \{0\} & [-R_T] & -[C_T]^{-1} \\ \{0\} & \{0\} & [R_T] & [0] \end{bmatrix} \begin{Bmatrix} \dot{x}(t) \\ x(t) \\ \{i(t)\} \\ \{q(t)\} \end{Bmatrix} + \begin{Bmatrix} F(t) - F_{ger}(t) \\ 0 \\ \{e(t)\} \\ \{0\} \end{Bmatrix} \right) \tag{6}$$

For the purpose of this work, the selected topology for the LPMA is classified as radial magnetization, internal magnet topology, slotted armature, and three-phase winding. Figure 4 illustrates the mentioned topology and Table 1 relates the dimensions and parameters of the electrical machine, used in this paper.

Table 1. Dimensions and parameters of the LPMA.

Dimension	Value	Description
h_{bi}	7.8 mm	Height of the back iron
h_c	22.5 mm	Height of the coils
h_m	5 mm	Height of the magnets
h_t	2 mm	Height of the teeth tips
g	1 mm	Airgap lenght
N	50	Number of windings
N_p	5	Number of pole-pairs facing the air gap
N_{ph}	3	Number of phases
N_s	15	Number of slots
N_{sp}	5	Number of slots per phase N_s/N_{ph}
R_{ag}	33.8 mm	Mean radius of the air gap
R_b	5 mm	Radius of the aluminium bar
R_i	34.3 mm	Inner radius of the stator
R_m	33.3 mm	Outer radius of the magnets
R_r	28.3 mm	Radius of the iron part of the rotor
R_s	66.6 mm	Outer radius of the stator
τ_m	32.3 mm	Magnet pitch
τ_p	32.3 mm	Pole pitch
τ_t	21.46 mm	Slot pitch
τ_{tt}	15.53 mm	Tooth width
τ_{tp}	19.1 mm	Width of the teeth tips
τ_w	3 mm	Width of the windings
τ_{wp}	64.6 mm	Winding pitch
τ_{ws}	1.18 mm	Width of the current sheets

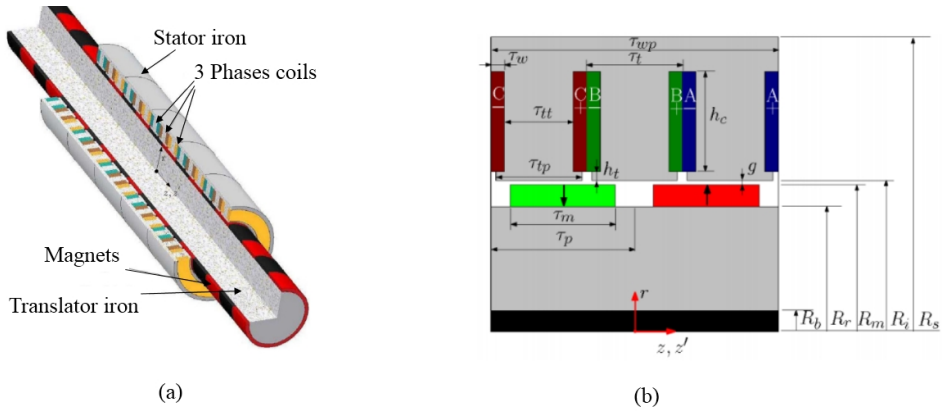

(a) (b)

Figure 4. (a) Topology of the LPMA select for this study. (b) One active part of LPMA with the relevant dimensions. Addapted from Gysen *et al.* (2010).

3. PARAMETRIC ANALYSIS

In order to understand the effect of change of the parameters which describe the mechanical and electrical systems over the performance of the LPMA, a series of simulations were done. The excitation force used in these simulations was a sinusoidal with known amplitude and frequency. The value of frequency was always equal to the natural frequency of the mechanical system. The initial conditions are both null for state variables and the simulated time was long enough to achieve the steady state condition. The results of the simulations were the electromotive voltage, the instantaneous current vector, the electromagnetic force, and the displacement and velocity of the translator. With these variables, the electrical power and the electromechanical efficiency are estimated.

3.1 Electromechanical efficiency and external circuit parameters

Figure 5 shows how the electromechanical efficiency varies with the value of the load resistance R_L. The mentioned figure also compares the curves of efficiency for all electric circuit models: the R model, the RL model, and the RLC model. The simulations were made considering the self- and mutual inductance of the LPMA associated with a 20 mH inductance, and with a 100 μC capacitance.

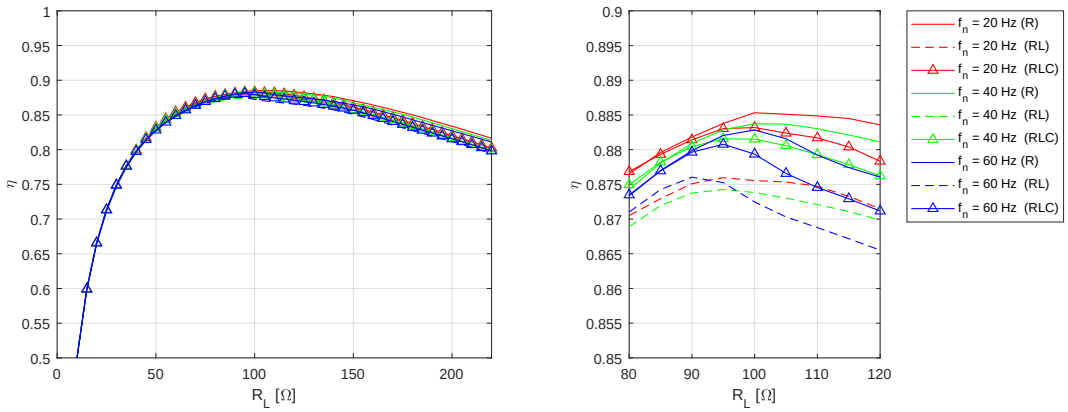

Figure 5. Curves of electromechanical efficiencies in function of the load resistance.

The efficiency of the generator depends on the load resistance. For small values of load resistance, higher current values can be produced however at the expense of limited displacement and velocity of the translator, which limits the the conversion of mechanical energy to electrical one. Otherwise, for higher load resistance values smaller damping coefficients are obtained and large powers can be harvested but at cost of low efficiencies. One can observe that there is a value of R_L, between 90 Ω and 110 Ω, for which the maximum efficiency is obtained. It is observed as well that the efficiency presents small variations due to the different value of natural frequency of the mechanical system. The R model obtained the highest values of efficiency, while the RL model the lowest, althought the differences are smaller than 1.5%.

Figure 6 shows how the electromechanical efficiency varies with the value of the inductance L_L. The value of the capacitance used in these simulations is 100 μC.

It is observed that higher values of the inductance lead to a sharp decrease in efficiency. The reason for this is that inductance limits the rate of current change, resulting in a smaller values of currents in each phase, hence smaller values

of converted energy.

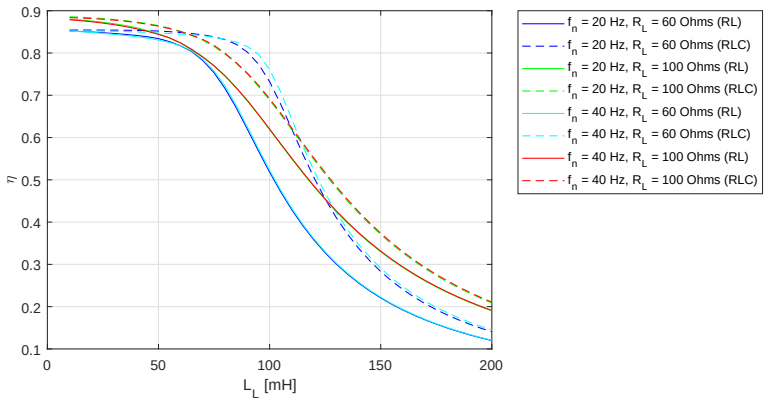

Figure 6. Curves of electromechanical efficiencies in function of the inductace L_L.

3.2 External circuit parameters and the electromagnetic force

Figure 7 shows the curves of the electromagnetic force for different values of the resistor R_L and inductance L_L. The natural frequency of the mechanical system is 20 Hz for all cases.

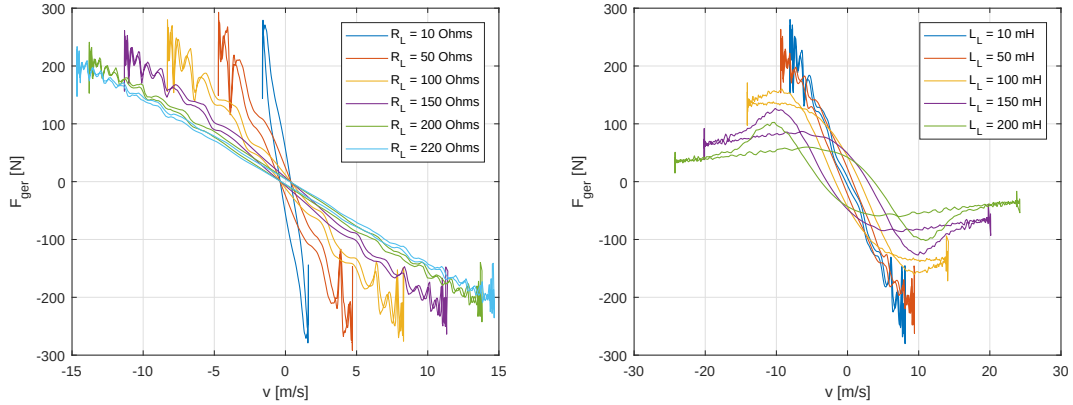

Figure 7. Curves of electromechanical induced force in function of: (a) the load resistor R_L; (b) the inductance L_L.

Based on the results, it can be observed that even though the different values of the circuit resistance, the overall curves of the electromagnetic force presents a behavior close to linear, although at the moments of higher velocities, a strong non-linearity is present. In contrast, the higher values of inductance result in a non-linear behavior independently of the velocity values as well in a limited maximum value of the analyzed force.

In the modelling process of systems with linear alternators, it is common to assume, with acceptable precision, that the load force induced by this equipment is proportional to the translator velocity, similarly to a ideal viscous damper. This proportional constant, defined as load constant or equivalent damping coefficient, is a parameter with which the dynamical behavior of this electric generator can be summarized.

The equivalent damping coefficient, c_{ger}, can be estimated by minimizing the objective function described in Eq. 7.

$$\hat{c}_{ger} = arg \min_{c_{ger}}(||c_{ger} \cdot \{\dot{x}\} - \{F_{ger}\}||) \tag{7}$$

Where $\{\dot{x}\}$ and $\{F_{ger}\}$ are the vectors of the results obtained in the steady-state condition.

Figure 8 illustrates how the equivalent damping coefficient varies for different values of load resistance and frequency. The curves for all electric circuit models are also compared.

The results shows that the equivalent damping coefficient presents a non-linear relation with the load resistance where increasing the resistance the smaller the equivalent damping. One can see that for the smaller values of R_L, the difference between the estimated c_{ger} are larger. It can be concluded that in this range of values, the estimated c_{ger} is also function of the frequency of the excitation force and of the inductance and capacitance of the electrical circuit. Ones should observe that low values of equivalent damping mean that less kinetical energy being converted in electrical energy.

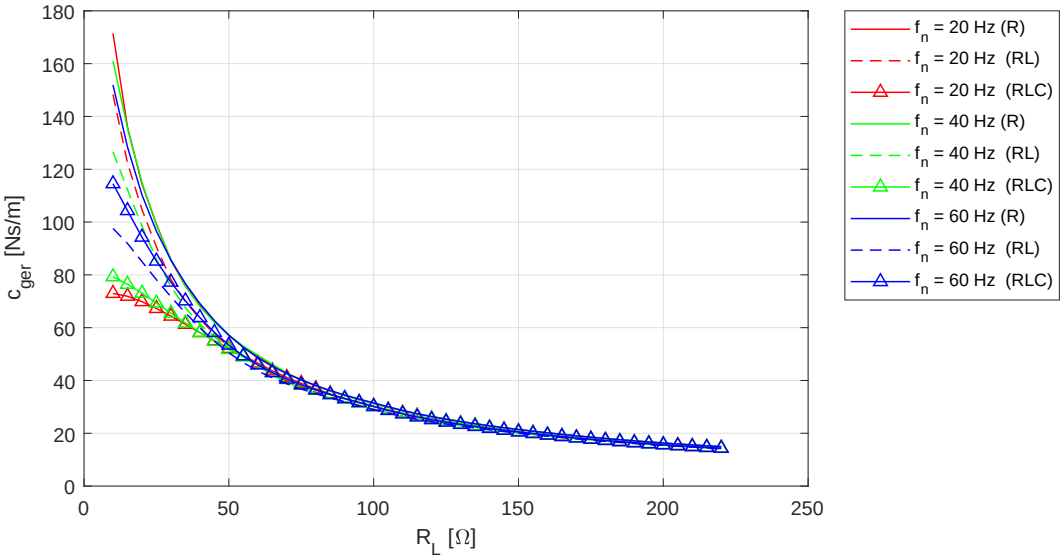

Figure 8. Curves of equivalent damping coefficient in function of the load resistance.

3.3 Electromechanical efficiency and the translator stroke

The design of a Linear Permanent Magnet Alternator requires a special observation related to the displacement amplitude of the translator. It is recommended that the stroke at the steady-state condition be the closest possible of the winding pitch for two reasons. First, to maintain the compactness of the machine. Second, to achieve the highest efficiency of the equipment (Boldea and Nasar, 1987).

The displacement amplitude of a 1 d.o.f. dynamical system depends on the amplitude and frequency of the excitation force. In order to maintain the stroke of the LPMA close to the desired value for different values of frequency, the amplitude of the excitation force can be estimated by Eq. (8).

$$F_o = 2 \cdot \pi \cdot c_{ger} \cdot \tau_{wp} \cdot f_n \tag{8}$$

Where c_{ger} and τ_{wp} are the equivalent damping coefficient and the winding pitch of the LPMA, respectively.

Figure 9 illustrates how the electromechanical efficiency varies with the stroke and winding pitch τ_{ws} ratio. The results used for this graph were obtained by varying the load resistance and the amplitude of the excitation force obtained via Eq. (8).

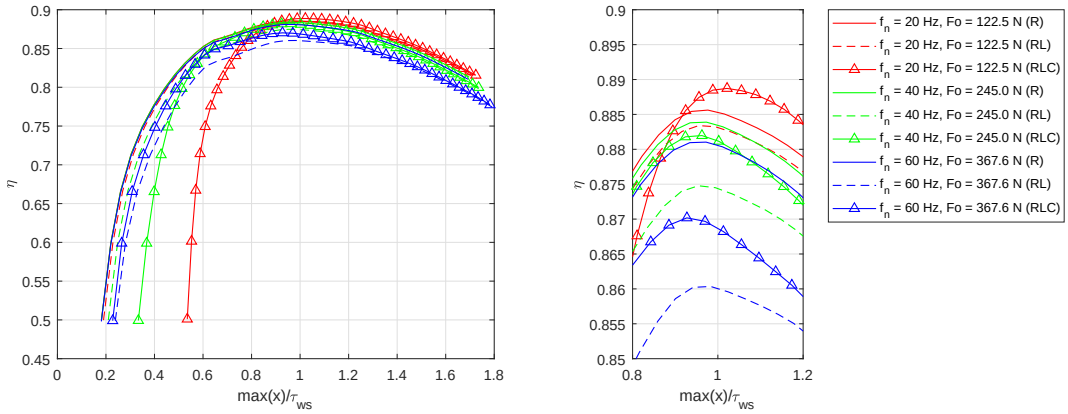

Figure 9. Curves of electromechanical efficiency in function of the stroke and winding pitch τ_{ws} ratio.

As described above, the maximum values of efficiency, independently of the natural frequency, occurs when the load resistance is close to $100\ \Omega$. For these cases, the stroke and winding pitch ratio were close to 1.0.

It is observed that the combined variation of the frequency and force amplitude of the excitation force resulted in slightly higher differences in the estimated maximum efficiencies. Comparing the results between different values of natural frequency for the same electrical circuit model, the maximum divergence obtained was close to $2.0\ \%$. Between different electrical circuit models for the same value of natural frequency, the highest difference value was too $2.0\ \%$.

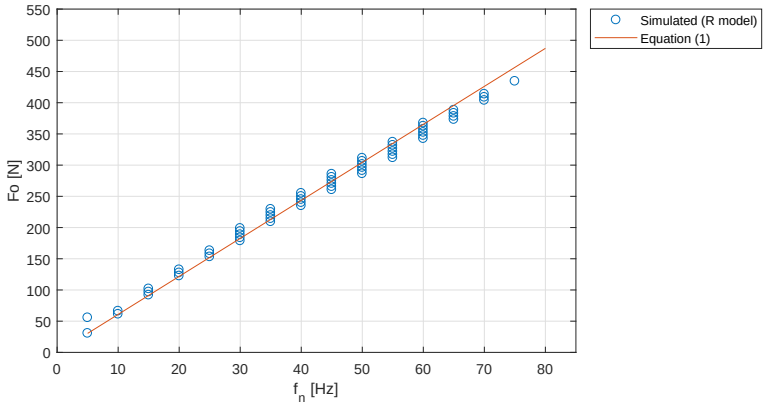

Figure 10. Curves of amplitude of the excitation force in function of the natural frequency f_n.

Figure 10 shows the amplitude of the excitation force for which the obtained displacement amplitude is close to the winding pitch of the LPMA ($32.5 \pm 2\ mm$) for different values of natural frequency of the mechanical system. Also, the simulation results are compared with the results obtained via Eq. (8).

Hence, for the dimensions and parameters of the LPMA used in this study cases, the region delimited by the circles in Fig. 10 can be considered as the desired region of operation of this equipment. If the designer select a wider region in Fig. 9 by determining a smaller minimum value of efficiency, the operating region area increases.

3.4 Influence of the excitation force type and suspension stiffness on the alternator performance

LPMA is proposed as electric generator which the prime movers are Stirling engines, linear internal combustion, and direct wave energy engines. Since the force driven by this type of prime movers over the system diverge from the sinusoidal curve, the type of force used as reference in the previous sections, a comparison between the estimated performance of the electric alternator for different types of force is done to clarify the influence of this feature over the evaluated performance.

Furthermore, in this comparison, one must consider other aspect of the model: the elastic element of the suspension. Occurs that the dynamical system works simarly to a mechanical filter, since the assembly of this elastic element with the translator results in a 1 d.o.f. vibratory system, and all frequencies are blocked but the one equals to the natural frequency of the system. Therefore, the presence or absence of the spring is also considered.

For the load resistance, excitation force amplitude and frequency equals to $100\ \Omega$, $250\ N$ and $40\ Hz$, respectively, the model was solved for three different excitation force curves: Sinusoidal, Triangular and Rectangular. Also, in order to verify the influence of the assembly of the elastic element and the translator, for each type of excitation force curve, the model was solved with $k = 0\ kN/m$ – representing the case where no elastic element is used – and with $k = 316\ kN/m$.

Figure 11 illustrates the results in the time domain, while Fig. 12 shows the magnitude of the displacement, velocity and electromagnetic force in the frequency domain, obtained with the Fast Fourier Transform.

First, the results in the time domain are analyzed. In the case that the translator is associated with the elastic element, one can observe that despite the difference between the excitation forces, only the amplitude of the evaluated variables distinguish. It can also be inferred that the amplitude is proportional to the RMS value of the excitation force.

The results of the simulations considering the absence of the spring show that the velocity curves of the translator are considerably different, depending on the type of the excitation force. In fact, for the case where the rectangular force was applied on the system, the resulting shape velocity curve was simillar to a triangular form. This fact may confirm that the system works as a mechanical filter, when the spring is associated with the translator.

Next, the results in the frequency domain are analyzed. In the case that the stiffness of the elastic element is not null, it is observed that the displacement and velocity presents a similar magnitude in frequency spectrum, regardless of the type of excitation force curve. For velocity spectrum, one can observe that for the rectangular and triangular forces, the magnitude of the third, fifth, and others harmonics are slightly bigger in comparison with the sinusoidal one, once that, the retangular and the triangular forces have these harmonics.

In the electromagnetic force spectrum, it is interesting to observe that third, fifth and others harmonic components present considerable amplitudes. Comparing the curves for the different types of force, the divergencies are stronger in the range between these harmonics frequencies.

For the case which the model is considered without the elastic element, the spectrum curves of the displacement presents the existence of the odds harmonics for the triangular and rectangular force curves, differently from the model with the spring. That can be also observed in the velocity spectrum curve. This fact confirms that the use of a spring associated to the translator results in a filter.

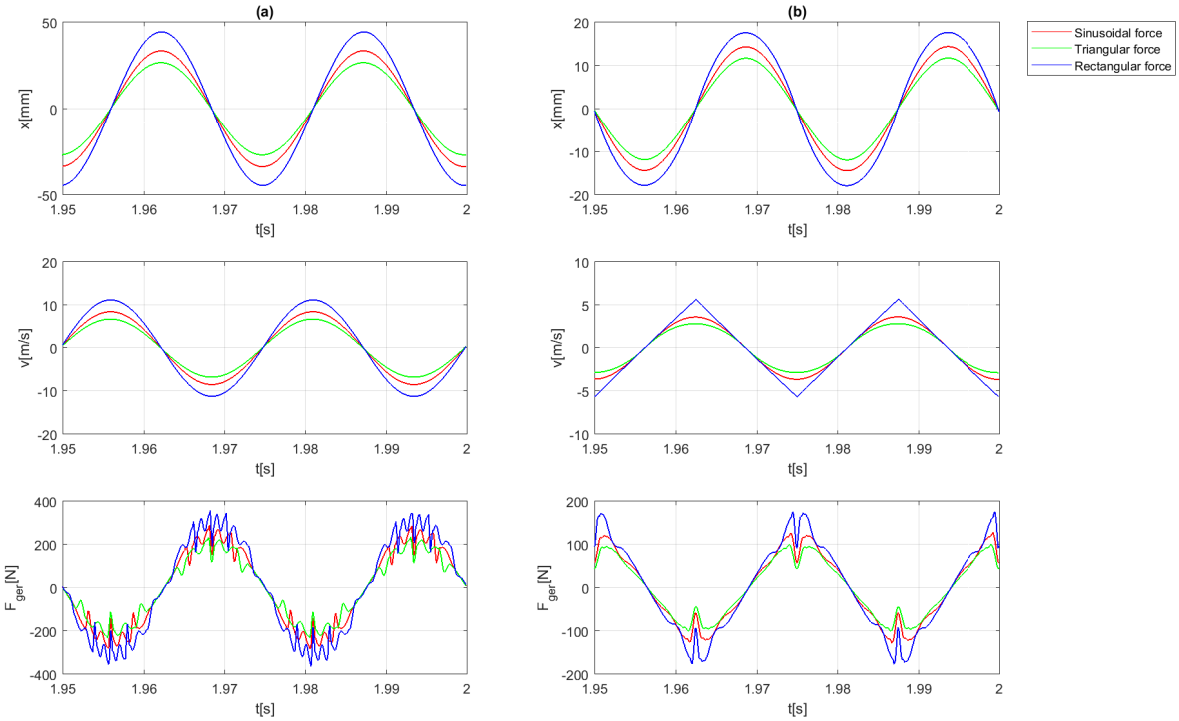

Figure 11. Displacement, velocity and electromagnetic force for different excitation force curves. (a) $k = 316\ kN/m$. (b) $k = 0\ kN/m$

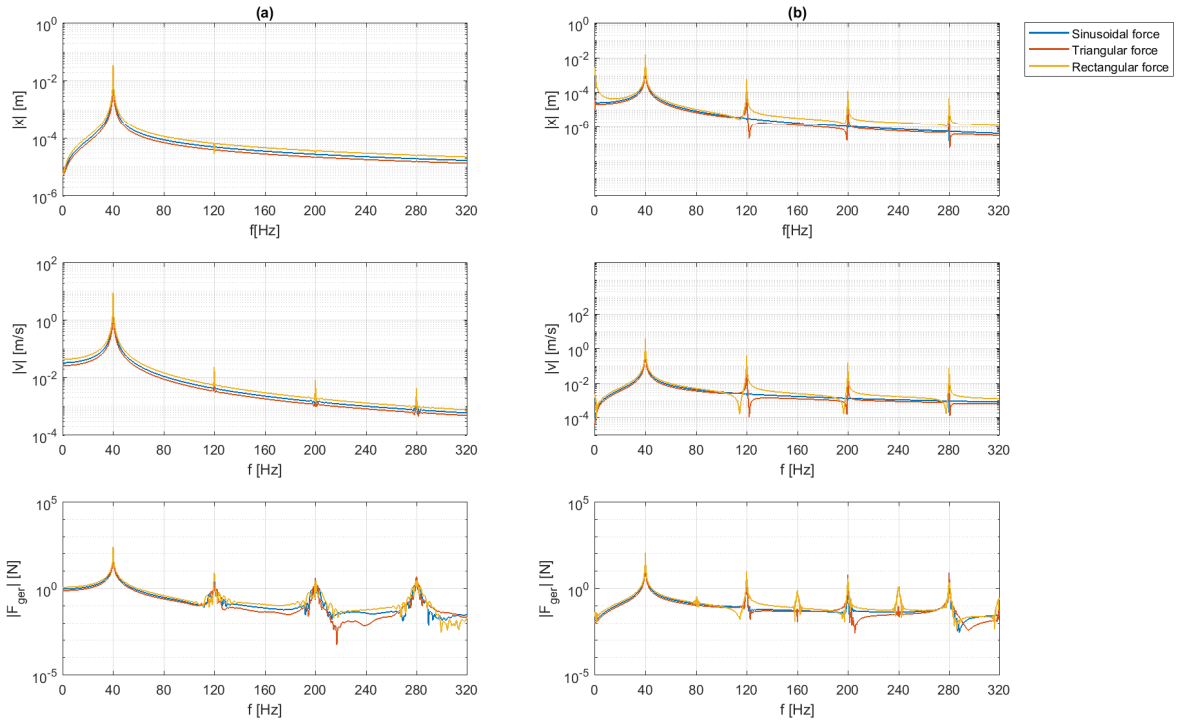

Figure 12. Magnitude of displacement, velocity and electromagnetic force in frequency domain for different excitation force curves. (a) $k = 316\ kN/m$. (b) $k = 0\ kN/m$

In the electromagnetic force spectrum, the third, fifth and others harmonic components are also present, although the diffenrences observed in the regions near the peaks, when compared with the case of the system with the spring. Also, for the cases which the triangular and rectangular force types were applied on the system, the existence of the second, forty and others evens harmonics.

Figures 13 and 14 show the efficiency and the stroke and winding pitch ratio in function of the frequency and type of the excitation force for the studied cases.

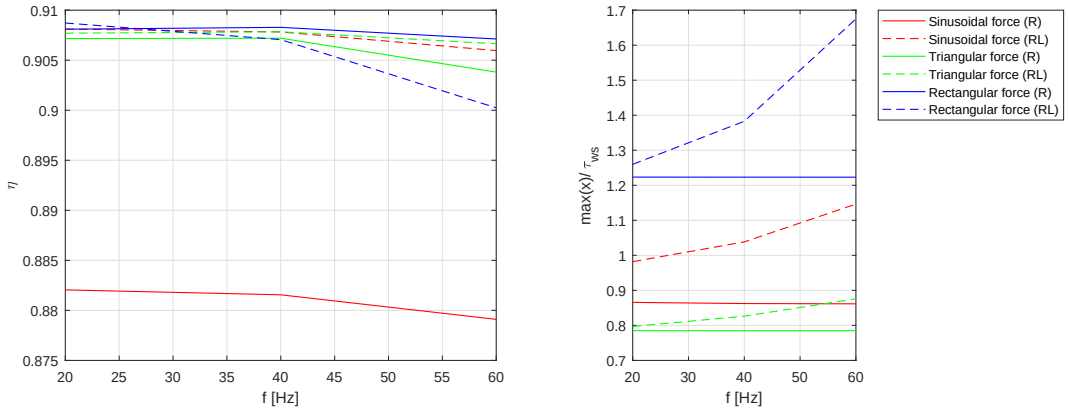

Figure 13. Efficiency and the stroke and winding pitch ratio in function of the frequency and type of the excitation force for the system with an elastic element.

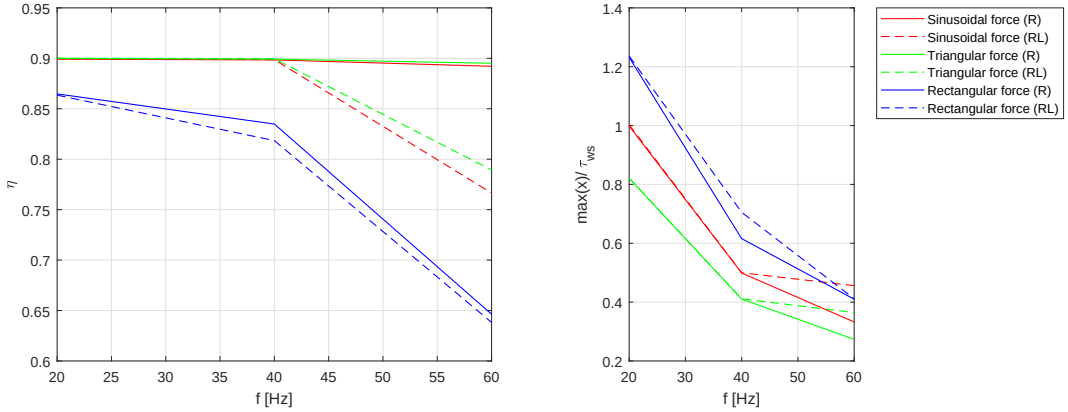

Figure 14. Efficiency and the stroke and winding pitch ratio in function of the frequency and type of the excitation force for the system without an elastic element.

The results show that the use of an elastic element as part of the system's suspension leads to higher values of efficiency, when greater values of excitation frequency are considered. It is also clear that the estimated efficiency of the electric equipment depends on the type of the excitation force. For the case of the system with a spring and a R-model,the lowest values of efficiency occurred for the sinusoidal excitation force. If the RL-model is considered, the rectangular force type achieved the worst performance results. For the system without the elastic element, the rectangular force type leaded to the lowest efficiency values, for both types of electric circuit models.

Thus, in a general scenario, the smoothest the excitation force curve is, the highest the efficiency. It may also be concluded, that the use of a elastic element leads to a more stable efficiency curve.

4. CONCLUSIONS

In this paper the Linear Permanent Magnet Altenator was described as a mass-spring vibration system submited to a external harmonic force. Given the design parameters of the electrical machine, the displacement, velocity, and accelaration of the translator, as well as the electromotive voltages, instantaneous currents, and electromagnetic force can be estimated in the time domain. With these results, the generated electrical power and the electromechanical efficiency of the analysed machine are determined.

In order to undestand the effect of change of the parameters which describe the mechanical and electrical systems over the performance of the LPMA, a parametric analysis was done. The results demonstrated that the electromechanical efficiency depends not only on the load resistance, but also on the circuit inductance, on the type of the excitation force, and on the presence or lack of the elastic element of the system's suspension.

The main conclusions were: For small values load resistance, the convertion of mechanical energy to electrical one is limited. As higher values of load resistance is used, the electromechanical efficiency arises until a maximum efficiency is achieved in a range between $90\ \Omega$ and $110\ \Omega$. Considering the circuit inductance, it was observed that the use of higher values of this component leads to a sharp decrease in efficiency due the limitation of rate of current change. The use of the spring associated to the translator affects the dynamic of the system considerably, by making it operate in a similar manner as a mechanical filter. It was also observed that the presence of the spring permits to achieve a higher values electromechanical efficiency at higher operating frequency and independently of excitation force type.

5. ACKNOWLEDGEMENTS

The authors gratefully acknowledge financial support from the CAPES/CNPq.

6. REFERENCES

Boldea, I. and Nasar, S.A., 1987. "Permanent-magnet linear alternators part ii: Design guidelines". *IEEE Transactions on Aerospace and electronic Systems*, , No. 1, pp. 79–82.

Gysen, B., Meessen, K., Paulides, J. and Lomonova, E., 2010. "General formulation of the electromagnetic field distribution in machines and devices using fourier analysis". *IEEE Transactions on Magnetics*, Vol. 46, No. 1, pp. 39–52.

Rodrigues, R.V., Santos, M.B. and Carvalho, S.R., 2019. "A model of a linear permanent magnet altenator for design and optimization: part i. modelling and validation". In *(COBEM), 2019 XXV International Congress of Mechanical Engineering*. ABCM.

7. RESPONSIBILITY NOTICE

The authors are the only responsible for the printed material included in this paper.